

UC Santa Barbara

UC Santa Barbara Previously Published Works

Title

Photochemical delivery of nitric oxide

Permalink

<https://escholarship.org/uc/item/1z13j4sv>

Author

Ford, Peter C

Publication Date

2013-11-01

DOI

10.1016/j.niox.2013.02.001

Peer reviewed

1 **Photochemical delivery of nitric oxide.**

2 Peter C. Ford

3 Department of Chemistry and Biochemistry, University of California, Santa Barbara
4 Santa Barbara, CA 93106-9510 USA; EMAIL: ford@chem.ucsb.edu

5
6 Abstract:

7 There remains considerable interest in developing methods for the targeted delivery of nitric
8 oxide and other small molecule bioregulators such as carbon monoxide to physiological targets.
9 One such strategy is to use a "caged" NO that is "uncaged" by excitation with light. Such
10 photochemical methods convey certain key advantages such as the ability to control the timing,
11 location and dosage of delivery, but also have some important disadvantages, such as the
12 relatively poor penetration of the ultraviolet and visible wavelengths often necessary for the
13 uncaging process. Presented here is an overview of ongoing studies in the author's laboratory
14 exploring new photochemical NO precursors including those with nanomaterial antennas
15 designed to enhance the effectiveness of these precursors with longer excitation wavelengths.

16

17

18

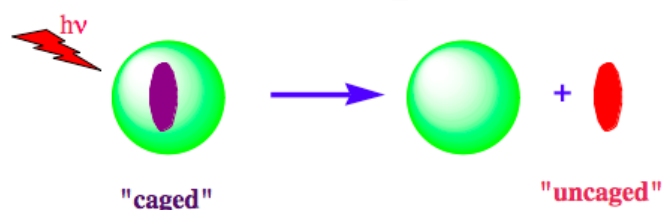
19 Keywords: nanomaterial, quantum dot, photochemistry, photoCORM, upconversion.

20

21 **Introduction:**

22 The purpose of this article is to provide an overview of studies in my laboratory relevant to
23 the delivery of small molecule bioregulators to physiological targets. Our approach and that of
24 others to more controlled, specific delivery is to develop stable compounds that release the
25 molecule in question only when triggered by an external signal, namely photo-excitation of an
26 appropriate precursor. The precursor is in principle inactive, hence the bioactive agent of interest
27 is "caged", but upon photoexcitation, the latter species is released ("uncaged") (Scheme 1).
28 Although we have focused primarily on the delivery of nitric oxide [1-3], these strategies should
29 apply to other chemotherapeutic molecules such as carbon monoxide, which has also drawn our
30 recent attention [4-6]. For CO, the term "photoCORM" (for photoactivated CO releasing moiety)
31 has been coined [4] to designate a photochemical CO precursor, and, while no such term has
32 caught on with NO precursors, one now hears "photoNORM" used occasionally. The advantage
33 of photo-activation is that the external signal allows one to define the *location* and *timing* of the
34 NO delivery. Furthermore, since the amount of photochemical reaction is a function of the
35 quantity of light delivered to the desired target, this allows one also to define the *dosage* of the
36 release. Although the present manuscript is focused largely upon our own studies, it should be
37 noted that there is a growing interest in applying photochemical methods to the uncaging of NO
38 [7-12] and CO [5,13-14] as well as other bioregulators [15].

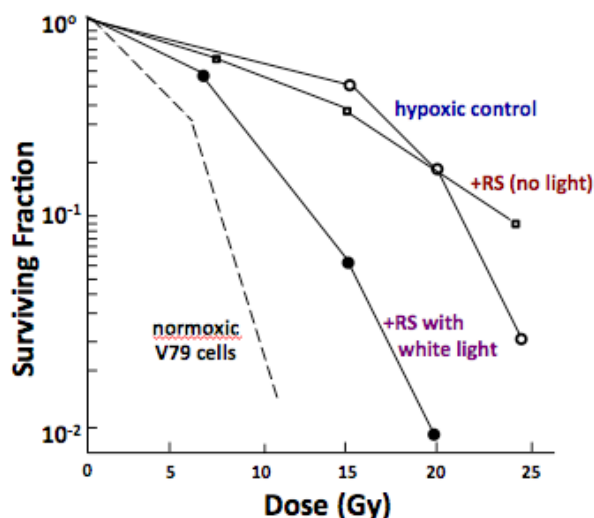
39 **Scheme 1:** Cartoon illustrating the photochemical uncaging of a bioactive substance which in the original "caged"
40 form (presumably some type of conjugate) is not active.



41
42 Various rationales for controlled NO delivery range include its cardiovascular effects,
43 antibacterial properties and potential roles in generating apoptosis in tumor cells. With regard to
44 cancer therapy, one problem is that, although high localized levels of NO can induce cell
45 apoptosis, low levels of NO may induce tumor growth instead [16]. Thus, it is essential to have
46 very careful control over the dosage delivered. In this context our interest in the
47 phototherapeutic NO delivery draws from the view that this should be synergistic with other

48 forms of treatment. For example, it has been shown that NO increases the sensitivity of tumor
49 cells to radiation therapy [17] and chemotherapy [18]. The hypoxic regions of malignant tumors
50 are much more radio-resistant than is normoxic tissue, therefore one should be able to reduce the
51 collateral damage from radiotherapy by developing strategies to increase the sensitivity of the
52 targeted tissue. Hypoxia radiation resistance may be alleviated by introducing a sensitizer and/or
53 a vasodilator to increase tissue oxygenation; both are roles played by NO. Radiation
54 sensitization requires NO concentrations near 1 μM [17], but vasodilation is triggered at much
55 lower concentrations of NO [19], so that even at very low concentrations, exogenously delivered
56 NO may indirectly enhance the radiation killing of tumor tissue.

57 An example of such radiation sensitization is illustrated in Figure 1. In this case, four
58 different samples of V-79 (Chinese hamster lung fibroblast cells) were subjected to γ -radiation
59 from a Co-60 source in an equivalent manner and the resulting cell viability evaluated [20]. One
60 cell sample was under aerobic conditions, and it is easily seen that less than 1% of the cells were
61 still viable after a γ -radiation dose of ~ 11 Gy. In contrast, hypoxic cells proved to be much more
62 resistant, with radiation doses exceeding 25 Gy to achieve a comparable effect. The same cells
63 incubated with a 500 μM solution of the photochemical NO donor Roussin's red salt
64 $\text{Na}_2[\text{Fe}_2\text{S}_2(\text{NO})_4]$ (RRS, see below) showed no enhancement of the radiation effect, but when a

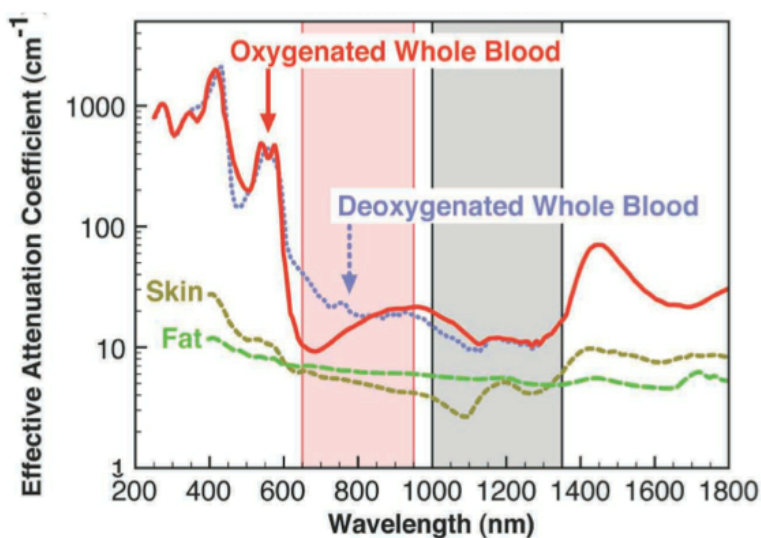


65
66 **Figure 1.** Survival of V79 Chinese hamster lung cells exposed to γ -radiation under hypoxic conditions without
67 (open circles) or with 500 mM Roussin's red salt (RS) under simultaneous irradiation with white light (closed
68 circles) or in the dark (open squares). The dashed line on the plot indicates the response of V79 cells exposed to γ -
69 radiation under normoxic conditions (WL refers to white light illumination. (Adapted with permission from ref. 20
70 Copyright 1997 American Chemical Society.)

71
72 comparable sample was also illuminated with light from a simple 35 mW projector, a marked
73 enhancement of the radiation damage was apparent. Given that these results paralleled those
74 observed when other NO donors were utilized, it was concluded that the photochemical release
75 of NO from the RRS is responsible for the observed sensitization [20].

76 With regard to carbon monoxide, it has long been known that CO is produced endogenously
77 by heme oxygenases, and there are newer developments indicating that endogenously and/or
78 exogenously produced CO may be cytoprotective during inflammation, promote wound healing,
79 and have signaling properties [for examples: 21-22]. In addition various CO donors have been
80 shown in animal studies to be effective in alleviating ischemia/reperfusion (I/R) injury in various
81 organs and tissues [for examples: 23-25].

82 Strategies for and problems with developing methodologies for photochemical CO and NO
83 release show certain parallels. One property desirable for a photochemical precursor would be
84 solubility in aqueous solution or (perhaps) in a medium such as aqueous dimethylsulfoxide
85 (DMSO) that is commonly used for drug delivery. Another would be reasonable stability in
86 aerated aqueous media at physiological temperatures and other conditions typical to living
87 organisms. A third would be photoreactivity at wavelengths where the transmission of light is
88 optimal (Figure 2) [26]. Penetration depth of light into tissue is strongly wavelength dependent.



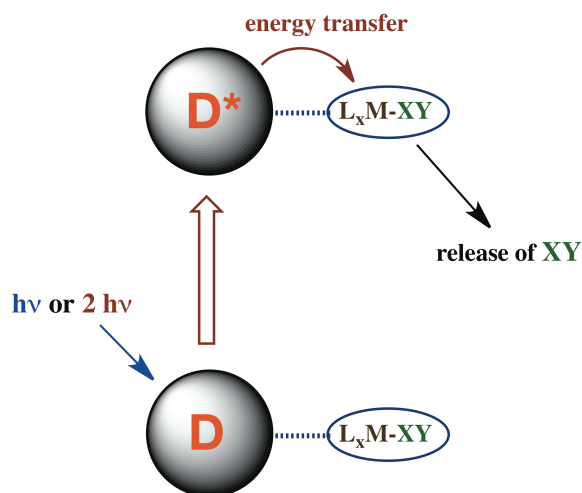
89
90 **Figure 2:** Absorption properties of various tissue components showing the windows in the near-infrared spectral
91 region (adapted from ref. 26 with permission from the Nature Publishing Group. Original figure provided by Dr.
92 A. Smith of Emory University)

93 It is shallow for ultraviolet light, but improves for longer visible wavelengths and tissue
94 penetration reaches its deepest values in the near infrared (NIR) spectral region (~700-1100 nm).

95 Photochemical activation at these longer wavelengths might be accomplished by using
96 antenna chromophores having high extinction coefficients at the desired wavelengths (Scheme
97 2). However, such an antenna can be an effective photosensitizer only if there are acceptor states
98 on the precursor molecule having the appropriate energies. A more ambitious approach would
99 be to utilize an antenna with a high two-photon excitation (TPE) cross-section in the NIR. For
100 such a system, excitation with a NIR laser could generate high-energy photosensitizer states that
101 can access reactive excited states of the photochemical precursor. We will discuss this approach
102 below.

103 It should be noted that, while these photochemical precursors are designed to release the
104 caged bioactive substance upon irradiation with light, a remaining molecular fragment is also
105 produced. These should be identified and characterized along with any secondary products
106 readily formed by subsequent reaction with the medium. Furthermore, the physiological
107 properties of these other photoproducts need to be examined to confirm whether the perceived
108 physiological effect is due to release of the caged species or to the unforeseen activity of other
109 species directly or indirectly generated. Lastly, as in the development of any new therapeutic
110 strategy, the acute and long-term toxicity of all these compounds must be evaluated.

111 **Scheme 2.** Single- or two-photon excitation of an antenna/photochemical precursor conjugate leading to release of
112 XY (CO or NO). D is the donor molecule acting as an antenna to absorb light give an excited state D* that
113 undergoes energy transfer to the acceptor molecule L_xM-XY, which is represented here as a metal complex that
114 releases X-Y after the energy transfer step.
115



116

117 In photochemical research, the efficiency noted above is called the *quantum yield* (Φ_P , eq. 1),
118 which is the amount (in moles) of the desired chemical reaction ΔP per Einstein of light absorbed
119 $\Delta h\nu$ (one Einstein = 6.023×10^{23} photons) by the photoactive precursor (eq. 1).

$$120 \quad \Phi_P = \Delta P / \Delta h\nu \quad (1)$$

121 For single photon excitation (SPE), ΔP should be a linear function of $\Delta h\nu$. Generally Φ_P is
122 determined for photoexcitation at a specific wavelength, since it may be wavelength dependent.

123 When the goal is to perturb a dynamic physiological system by photochemical release of a
124 bioactive substance, the uncaging *rate* may be of greater interest. This is defined by (eq. 2),

$$125 \quad d[P]/dt = \Phi_P I_a \quad (2)$$

126 where $d[P]/dt$ is the rate product formation in moles per unit time per unit volume and I_a is the
127 intensity of the light absorbed by the precursor in Einsteins per unit time per unit volume at the
128 excitation wavelength. I_a is a function both of the incident light intensity I_0 and the ability of the
129 compound to absorb at the wavelength of excitation. For a solution phase system where the
130 photoreactant is the only species absorbing the incident light,

$$131 \quad I_a = I_0(1 - 10^{-\text{Abs}(\lambda)}) \quad (3)$$

132 where $\text{Abs}(\lambda)$ is the solution absorbance at the excitation wavelength λ_{irr} and equals the product
133 of the molar concentration of the photoactive species (c), the molar extinction coefficient (ϵ_λ , in
134 $\text{L moles}^{-1} \text{cm}^{-1}$) at the wavelength λ and the path-length of the solution cell (in cm). Thus, the
135 rate of photoproduct formation under SPE at a particular wavelength will be directly proportional
136 to I_0 and to Φ_P and will be a more complex function of c and ϵ_λ . In this context, efficient
137 photochemical delivery to physiological targets should be more favorable with precursors that
138 absorb strongly at the desired excitation wavelength(s) λ_{ex} . If the product $c \times \epsilon_\lambda$ is sufficiently
139 large, all the light is absorbed and the photoreaction rate becomes independent of both terms.
140 However, this scenario is unlikely in a targeted tissue, and absorption by other chromophores or
141 scattering of the light beam can have a significant effect on I_a . When polychromatic light is used,
142 the photochemical rate is the integral of $\Phi_P \times I_a$ over the excitation wavelengths, noting that Φ_P
143 may be, and I_a certainly will be, functions of λ_{irr} .

144 The ensuing sections will discuss first the use of typical single photon excitation methods
 145 with various nitric oxide precursors ("caged NO"), including those with antenna chromophores
 146 to enhance the absorption of light. We will then examine the potential applications of multi-
 147 photon excitation methods to facilitate the photochemistry of such precursors using tissue
 148 penetrating near infrared (NIR) light.

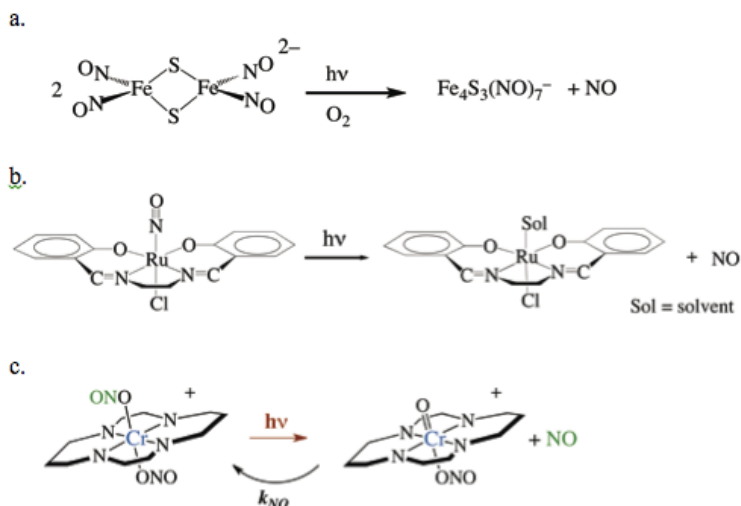
149

150 **Photochemical NO precursors:**

151 Scheme 3 illustrates several representative types of transition metal complexes that release
 152 NO upon photoexcitation. Two of these (a and b) are metal nitrosyls, where the nitric oxide is
 153 caged by coordination to a transition metal center [20,27]. For such complexes, a commonly
 154 observed photochemical process is cleavage of the metal-NO bond to give neutral NO (rather

155 **Scheme 3.** Examples of photochemical NO release from compounds representative of those under study. a.
 156 Roussin's red salt anion. b. A ruthenium salen nitrosyl complex. c. The Cr(III) nitrito complex *trans*-
 157 Cr(cyclam)(ONO)₂⁺ (cyclam = 1,4,8,11-tetrazacyclotetradecane)

158



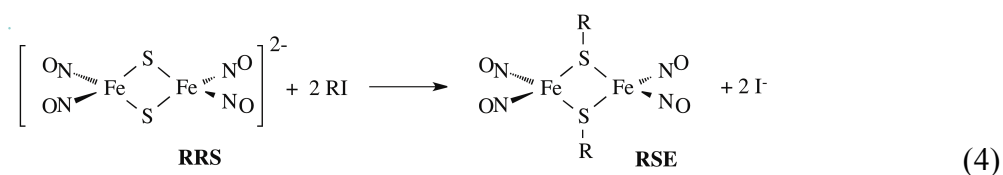
159

160

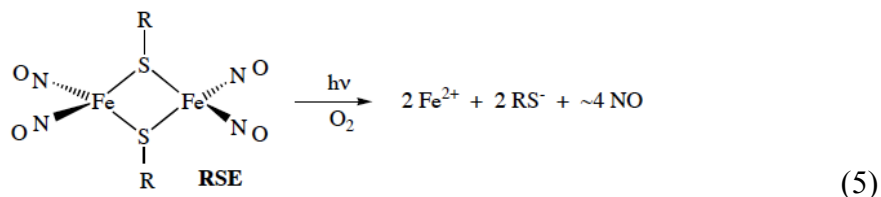
161

162 than the ionic species NO⁻ or NO⁺). The third example is an O-nitrito complex [28] where the
 163 NO is caged by bonding to another oxygen. In this case, NO is released by homolytic cleavage of
 164 the MO-NO bond. Since the nitrogen of nitrite ion is formally in the +3 oxidation state and that
 165 of NO is formally +2, the extra electron must come from the metal center. Thus, for the example
 166 shown, the release of NO is accompanied by the oxidation of the metal, in this case a
 167 chromium(III).

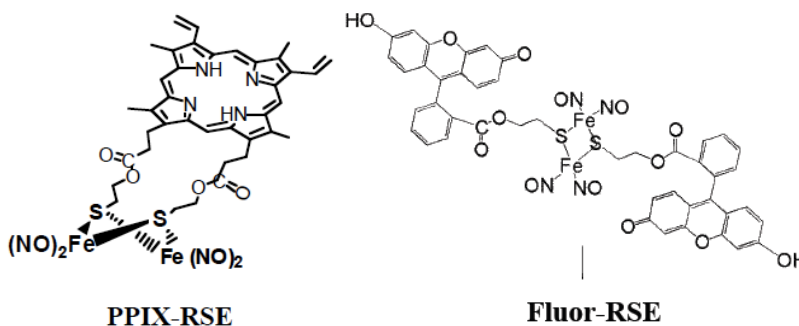
168 The iron sulfur nitrosyl anionic cluster, Rousin's red salt anion (RRS) was the NO precursor
 169 used to demonstrate that photochemically released NO enhances the ability of γ -radiation to kill
 170 hypoxic cultured cells as illustrated in Figure 1. RRS absorbs broadly in the visible and this
 171 radiation sensitization experiment proved quite successful using a simple slide projector as the
 172 white light source. However, RRS is only modestly stable in aerobic aqueous media, so in
 173 search of more stable analogs, our studies turned to the red salt esters (RSE) that are prepared by
 174 the reaction shown in eq. 4.



176 These RSE, even with simple ligands such as a benzyl or ethyl group, qualitatively displayed
 177 greater stability as well as more efficient NO release, since photolysis in aerated aqueous
 178 solution led to the release of all four NO's (eq. 5) [29].

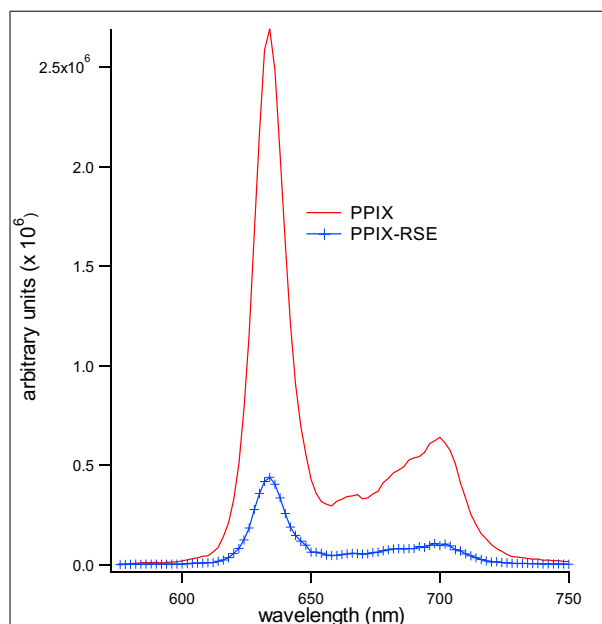


180 Furthermore, variations of this synthetic procedure could be used to build RSE's with R-
 181 groups having strongly absorbing chromophores. Two such examples are PPIX-RSE and Fluor-
 182 RSE, where the pendant groups are derivatives of protoporphyrin XI [30] and of fluorescein [31],
 183 respectively. These pendant chromophores are much more efficient at gathering light than is the
 184 $\text{Fe}_2\text{S}_2(\text{NO})_4$ cluster itself, hence they can serve as antennas that are first excited then undergo
 185 energy transfer to the cluster to photosensitize NO release.



186

187 The photochemistry of both PPIX-RSE and Fluor-RSE clearly demonstrate this antenna
188 effect. For example, dilute solutions (10 μM), photo-decomposition of the PPIX-RSE conjugate
189 excited at longer visible wavelengths (λ_{irr} 546 nm) occurred at much higher rates than did the
190 simpler ester $\text{Fe}_2(\mu\text{-SEt})_2(\text{NO})_4$ (Et-RSE) under otherwise identical conditions [30]. The
191 enhanced *rate* of NO release was largely attributed to the more efficient light absorption (I_a) by
192 the tethered PPIX owing to the strong porphyrin Q-bands in this region. In addition, the
193 fluorescence that is characteristic of the PPIX chromophore was largely quenched (Figure 3),
194 presumably as the result of energy transfer to the RRS cluster. Thus, attaching an antenna to the
195 red salt cluster enhances *the rate* of NO production via the visible light photoreaction as
196 intended. However, *the quantum yields* for both PPIX-RSE and Et-RSE are relatively low at this
197 excitation wavelength.



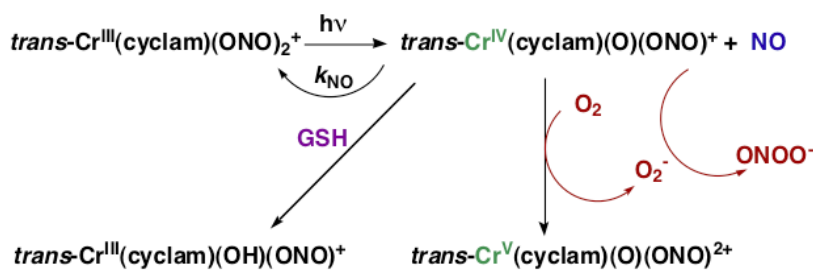
198 **Figure 3.** The fluorescence spectra of free PPIX and the red salt ester PPIX-RSE at comparable concentrations and
199 under identical conditions, showing that the fluorescence from the latter is about 85% quenched by attachment to the
200 Fe/S/NO cluster. Emission lifetime measurements confirm that this quenching is likely due to energy transfer to the
201 cluster. (Reprinted with permission from ref 30. Copyright 2004, American Chemical Society.)

202 Fluor-RSE with two pendant fluorescein dye units represents the second generation of such
203 Roussin's esters. This compound is moderately soluble in buffered aqueous solutions, and like
204 PPIX-RSE, the characteristic fluorescence of the antennas is $\sim 85\%$ quenched upon linking to the
205 Fe/S/NO cluster. The photochemistry of Fluor-RSE in aqueous media parallels that seen for
206 other esters. Consistent with eq. 5, all four NOs were released with a Φ_{NO} of 0.014 when
207 irradiated at 436 nm [31].

208 The metal nitrito complex $trans\text{-Cr}(\text{cyclam})(\text{ONO})_2^+$ (called "CrONO" in our lab) has several
 209 attractive features as a potential therapeutic photochemical NO precursor. First, it is thermally
 210 stable under physiologically relevant conditions (pH 7.4, normoxic aqueous buffer at 37 °C) and
 211 limited cell culture studies indicated no toxicity [32]. Second, CrONO is photoactive, and
 212 displays a substantial quantum yield for the release of NO according to the reaction shown in
 213 Scheme 3c over the wavelength range 365-536 nm. The quantum yield measured by spectral
 214 changes is 0.25-0.30 moles Einstein⁻¹ and is essentially independent of the excitation wavelength
 215 λ_{ex} . Direct measurement of NO release using a Sievers Nitric Oxide Analyzer (NOA) gave an
 216 equivalent quantum yield ($\Phi_{\text{NO}} = 0.25$) when the trapping agent was GSH. However, the visible
 217 range absorption bands leading to this photochemistry are metal centered d-d bands (sometimes
 218 called ligand field bands) and these have very low extinction coefficients ϵ_{λ} , since they represent
 219 symmetry forbidden transitions. As a consequence, the rates of NO generation are relatively low
 220 unless the concentration of CrONO and/or the intensity of the excitation light source is high (see
 221 eqs. 2 and 3)

222 Another feature of the CrONO system is that there is a relatively fast back reaction ($k_{\text{NO}} = 3.1$
 223 $\times 10^6 \text{ M}^{-1} \text{ s}^{-1}$ in 298 K aqueous solution) to regenerate the coordinated nitrite [28]. In such a case,
 224 it may be necessary to trap the metal-containing fragment in order to ensure a substantial net
 225 yield of NO release. The $\text{Cr}^{\text{IV}}(\text{O})$ intermediate formed by the reaction illustrated in Scheme 3c is
 226 subject to both oxidative and reductive trapping (Scheme 4) [32,33]. When either an oxidant
 227 such as O_2 or a reductant such as glutathione (GSH) is present to trap the Cr(IV) intermediate,
 228 permanent photochemistry is observed. Thus CrONO is an effective NO donor under a variety of
 229 conditions, but should be especially effective in hypoxic tissue where the Cr(IV) would be

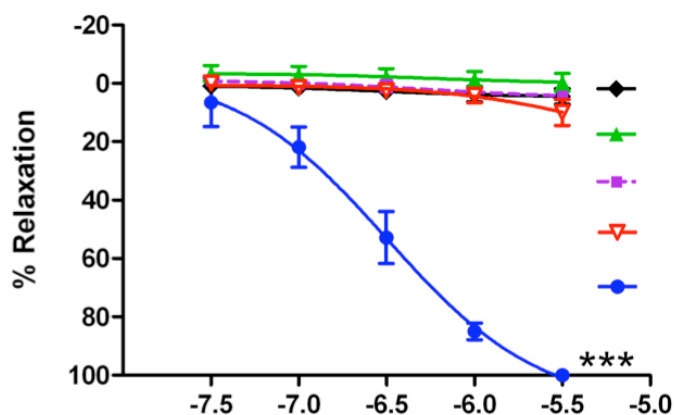
230 **Scheme 4:** The reversible labilization of NO from CrONO. The net production of NO is effected by the trapping of
 231 the Cr(IV) intermediate by oxygen in aerobic media or by GSH in a more reducing environments. The reaction with
 232 O_2 in aerobic media is complicated by the formation of O_2^- which can trap a substantial fraction of the NO to give
 233 peroxoxynitrite (adapted from ref 33).



234

235 trapped by GSH or other reductants.

236 Despite the small molar extinction coefficients of CrONO, it is notable that the NO
237 photochemically released from even quite dilute solutions is sufficient to activate the enzyme
238 soluble guanylyl cyclase (s-GC) and to effect vasorelaxation in porcine arteries (Figure 4). Both
239 phenomena, of course, reflect the great sensitivity of s-GC activation to NO [19]; nonetheless
240 these observations demonstrate the potential applicability of the photochemical technique for
241 delivering bioactive molecules to desired targets. For example, the experiments summarized by
242 Figure 4 clearly show that the porcine arterial ring relaxation can be attributed to NO generated
243 by photolysis of CrONO, not to other photoproducts nor to the complex itself. Under these
244 conditions, the IC₅₀ for solutions of CrONO is ~ 320 nM [33].



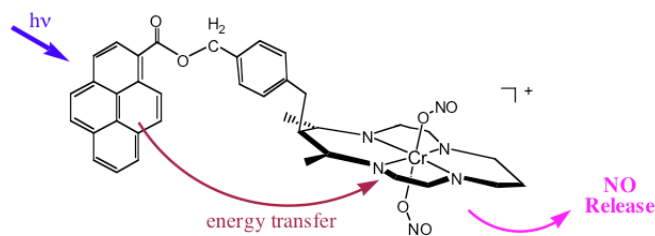
245
246 **Figure 4:** Effect of CrONO on vasorelaxation in endothelium-denuded porcine coronary arterial rings. Black
247 diamonds: in the dark; Green triangles: ambient light; Blue circles: exposed to 470 nm LED; . Red open triangles:
248 vasodilator effect of light activated CrONO was abolished the sGC inhibitor, ODQ is present. Purple squares: a
249 product solution of photolyzed CrONO had no effect in the dark. (Figure adapted from ref. 33.)

250
251 Thus, CrONO is a compound that satisfies most criteria for a photochemical NO precursor
252 with the exception of its very low absorptions at desired longer visible wavelengths. To address
253 this limitation, we have therefore turned our efforts to attaching various chromophores to
254 CrONO-like systems to serve as antennas for enhancing light absorption and increasing rates of
255 photo-induced NO production. Our first studies in that regard focused on organic dyes linked via
256 the macrocyclic cyclam ring, such as illustrated by Scheme 5 (top). Such conjugates clearly
257 demonstrate that attachment of such a dye increases the rate of NO production from dilute
258 solutions owing to the greater absorption cross sections of the pendant antenna [34].

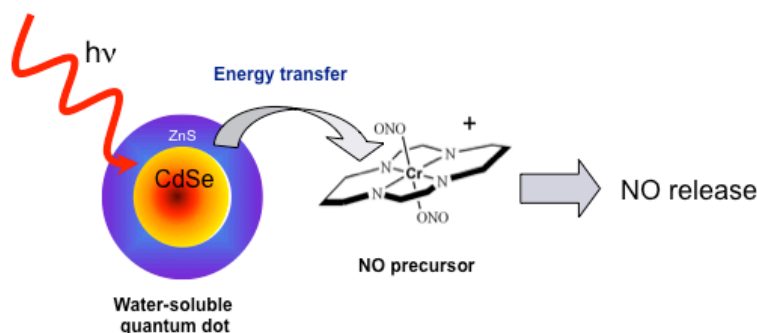
259

260 **Scheme 5.** *Top:* Illustration of a pendant pyrene type chromophore acting as an antenna to collect light and
261 photosensitize the release of NO from a CrONO type center [32]. *Bottom:* Analogous photosensitization of NO
262 release from CrONO using a water-soluble CdSe:ZnS core:shell semiconductor quantum dot as the antenna [34-36].

263



264



265 It was in this context that we decided to consider semiconductor quantum dots (QDs) as
266 potential photosensitizers. The first system we explored consisted of CdSe:ZnS core:shell QDs
267 with a core diameter of ~ 3.8 nm that had been ligand exchanged to decorate the surface with
268 dihydrolipoic acid (DHLA) in order to impart water solubility at physiological pH [35,36]. In
269 aqueous solution, these QDs displayed a photoluminescence (PL) centered at 570 nm, that was
270 progressively quenched with increasing concentrations of added CrONO. More importantly,
271 when a solution was prepared containing these QDs (100 nM) and CrONO (200 μ M) and was
272 photolyzed, substantially more NO was generated than from analogous solutions containing only
273 CrONO at the same concentration. Subsequent studies confirmed that both the PL quenching
274 and the sensitized NO production can be attributed to an energy transfer mechanism from the
275 excited QDs to CrONO (Scheme 5 bottom) [36]. The interaction between the CrONO cations
276 and the water-soluble QDs would appear to involve electrostatic assemblies formed by ion
277 pairing at the anionic QD surfaces. We do not expect such assemblies to be stable under
278 physiological conditions, hence we are developing synthetic protocols to attach CrONO and
279 other photochemical nitric oxide precursors to the QD surfaces via strong covalent bonds.

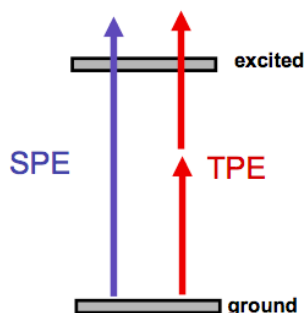
280

281 **Multi-photon excitation using near-infra red light.**

282 The reactive excited states of otherwise attractive precursors are often too high in energy to
283 be accessed by typical single photon excitation (SPE) using excitation at longer visible
284 wavelengths or in the NIR therapeutic window. In such a case, even the attachment of an antenna
285 with strong absorption bands does not help, since there would be insufficient energy to sensitize
286 the population of these high energy states. In principle this limitation can be addressed by using
287 multi-photon excitation, where the summed energy of several NIR quanta are sufficient to
288 generate the energies necessary to trigger the desired uncaging. Two different multi-photon
289 excitation approaches have been explored in our laboratory: (a) two photon excitation (TPE)
290 which involves simultaneous absorption of two quanta of light, and (b) energy transfer
291 upconversion (ETU) which can be obtained by sequential absorption processes. TPE is
292 illustrated in Scheme 6, while ETU is discussed below

293 The rates of photochemical processes initiated by simultaneous or sequential multi-photon
294 absorption processes typically will have a non-linear dependence on the light intensity I_o , which
295 is different from the behavior of SPE stimulated processes (eqs. 2 & 3). For example, the
296 probability of TPE is proportional to I^2 , the square of the incident light intensity, if a single
297 source is utilized. Thus, TPE induced photoreaction will be fastest at the focal plane of the light
298 source. This therefore offers the possibility of 3-D spatial resolution, a property that is
299 extensively exploited in imaging [37,38] and offers interesting possibilities in phototherapy [39].

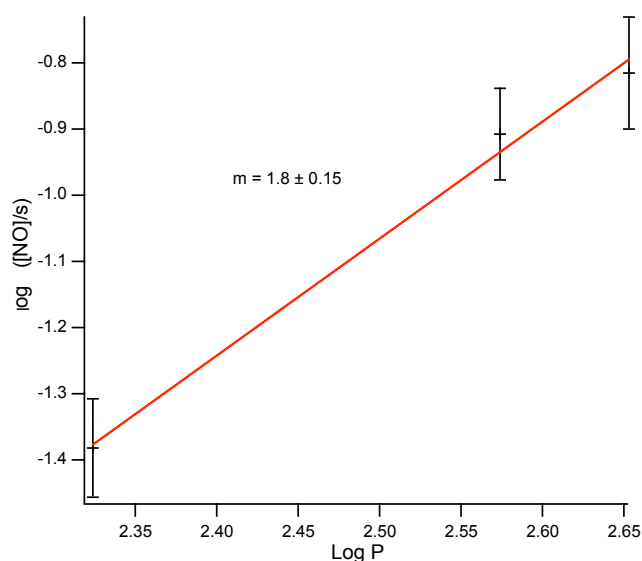
300 **Scheme 6.** TPE model for achieving higher energy excited states (ES) using multi-photon excitation. TPE involves
301 simultaneous absorption of two photons to generate an ES (E_2) having the summed energy of the two photons. The
302 resulting ES may undergo emission, may react to give products or undergo energy transfer to another chromophore.



303
304 *Two photon excitation and absorption:* The selection rules for TPE are different from those
305 for SPE; the former is allowed only between two states that have the same parity, while the latter

306 requires a parity change. Chromophores with high two photon absorption cross sections in the
307 NIR excitation region include extensively π -conjugated molecules especially that are
308 quadrupolar with electron-donor and -acceptor units arranged symmetrically with respect to the
309 center [40,41]. Semi-conductor quantum dots are also TPE chromophores with two photon
310 absorption cross sections as large as 10^4 GM seen for the commonly studied cadmium selenide
311 core or CdSe/ZnS core/shell QDs [42,43].¹

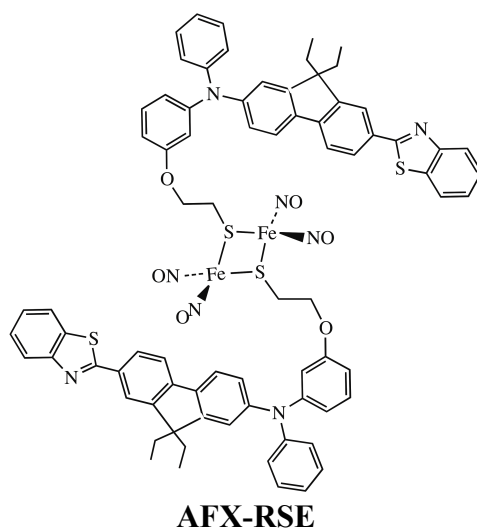
312 Our first TPE study involved the Roussin's red salt ester PPIX-RSE that we had previously
313 shown to be photoactive to NO release when subjected to SPE at mid-visible wavelengths [29].
314 Wecksler et al tested this possibility by subjecting a solution of PPIX-RSE to 810 nm NIR
315 excitation with 100 fs pulses from a Ti/sapphire laser [44]. These intense NIR pulses led to weak
316 phosphorescence from PPIX-RSE (λ_{\max} 632 nm) accompanied by NO generation. Both the NO
317 release and emission provided clear evidence that the higher energy ESs responsible for these
318 phenomena were being populated by multiphoton excitation, even though the two photon
319 absorption cross-section (δ) of PPIX is known to be quite low (~ 2 GM).



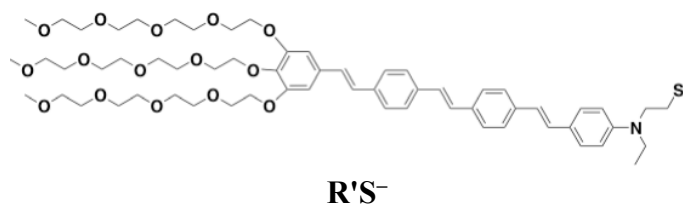
320
321 **Figure 5.** TPE of Fluor-RSE. Log [NO]/s versus Log P plot, where [NO]/s is the concentration of NO released in
322 30 s under 800 nm excitation, and P is the average power (in megawatts) of the pulsed laser (100 fs pulses at 80
323 MHz) which is proportional to the pulse intensity I . The slope = 1.8 ± 0.15 . (adapted from ref. 31)
324

¹ The GM is the unit of two photon cross sections, and $1 \text{ GM} = 10^{-50} \text{ cm}^4 \text{ s photon}^{-1}$. This is named in honor of Maria Goeppert-Mayer, who first proposed theoretically the concept of two photon excitation, a concept that was not confirmed until decades later.

325 Wecksler extended these studies to two other red salt esters, Fluor-RSE and AFX-RSE. In
326 both cases the pendant dyes have been shown to have much higher δ values [31,45]. In both
327 cases, the fluorescence properties of the excited state species formed after TPE at 800 nm were
328 the same as those observed upon SPE at 436 nm, indicated that the same states are formed
329 regardless of the method of excitation. In each case, the fluorescence was markedly attenuated
330 from that of analogous chromophores without the Fe/S/NO cluster, and this was accompanied by
331 NO release. When Fluor-RSE was irradiated with 800 nm light from the ultrafast laser system, a
332 log/log plot of the NO generated vs. the excitation intensity was linear with a slope of 1.8 ± 0.2
333 (Figure 5), consistent with the squared dependence on excitation intensity as expected for a
334 photochemical process initiated by TPE [31].

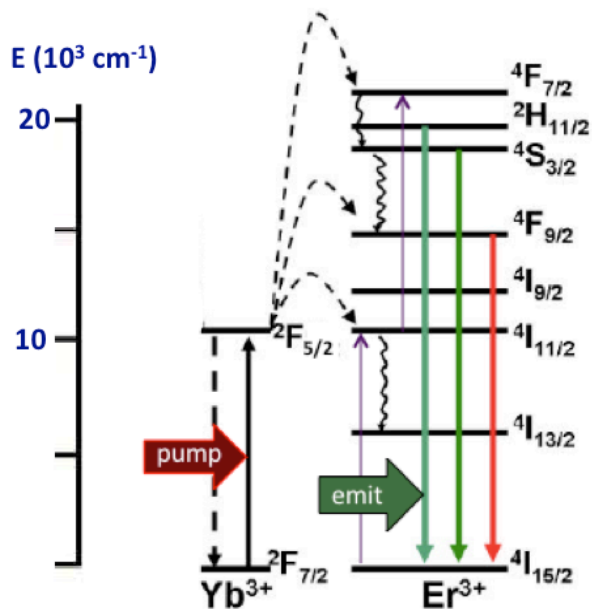


338 A subsequent study by Prasad and coworkers [46] described another RSE derivative
339 $\text{Fe}_2(\text{NO})_4(\mu\text{-SR}')_2$, where R'S- is the chromophore oligo-phenylene vinylene amine with a large
340 δ , conjugated to tetra(ethylene glycol) ethers to improve aqueous solubility. Both SPE at 365 nm
341 and TPE at 775 nm led to NO release as well as light dependent cytotoxicity in Hela and Cos-7
342 cancer cell cultures. As expected the magnitude of the effect was greater in the SPE experiments
343 owing to the greater flux of NO generated with direct UV excitation, although this advantage



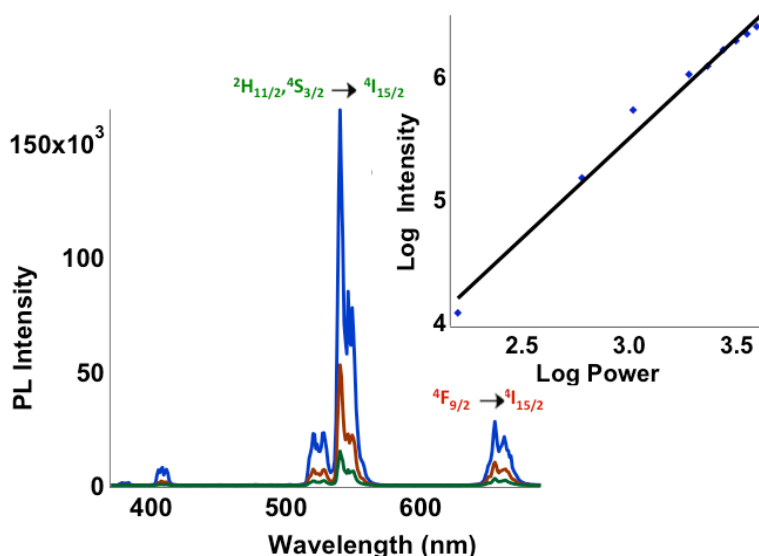
346 would be attenuated in tissue systems owing to the dramatically different transmission properties
 347 of the two wavelengths. This and the other studies with Roussin's red salt esters suggest the
 348 feasibility of using two photon excitation techniques for the delivery of NO to physiological
 349 sites, although much more needs to be done.

350 *NO uncaging using Ln^{III}-doped NIR upconverting nanoparticles (UCNPs):* Energy transfer
 351 upconversion (ETU) involving the sequential absorption of photons is another process that is
 352 nonlinear with regard to the intensity of the excitation source. Luminescent UCNPs based on the
 353 lanthanoid ions can be used in such devices owing to the relatively long lifetimes of the f-f
 354 excited states [47]. Typically, a Ln^{III} ion such as Yb³⁺ is the sensitizer that absorbs the NIR light
 355 and transfers this energy to an acceptor Ln^{III} ion such as Er³⁺, Tb³⁺, or Tm³⁺ as illustrated in
 356 Figure 6 [48]. Continued excitation of the sensitizer Yb³⁺ leads to further energy transfer to the
 357 long-lived acceptor states to populate new, higher energy states from which emission (or
 358 emissions) occurs at considerably shorter wavelengths than the initial NIR source. The absolute
 359 and relative intensities of the upconverted visible or ultraviolet wavelength emissions will
 360 depend nonlinearly on the intensity of the pumping process.



361
 362 **Figure 6.** Energy transfer upconversion (ETU) model for achieving higher energy excited states using multi-photon
 363 excitation. Pumping the sensitizer center (Yb³⁺) with 980 nm NIR light gives an ES (²F_{5/2}) that can undergo energy
 364 transfer to an acceptor (Er³⁺) to give a long lived ES. Continued excitation of the sensitizer Yb³⁺ followed by energy
 365 transfer to Er³⁺ gives the higher energy ES from which several visible range emissions occur. Figure adapted from
 366 ref. 48.

367 The energies of 4f-4f electronic transitions are primarily defined by spin and electronic
368 repulsion terms and show little sensitivity to the chemical environments of the Ln^{III} cations [45].
369 However, 4f-4f excited state lifetimes are quite sensitive to the environment, since collisions and
370 vibronic coupling contribute strongly to non-radiative deactivation. If an appropriate solid matrix
371 is used, collisional contributions are eliminated and the phonon-coupling pathways are
372 suppressed to give longer lifetimes and stronger emissions [49]. Various host crystals such as
373 NaGdF₄, NaYF₄, LaPO₄, YF₃, or Y₂O₃ have been used, and the β-phase (hexagonal) NaYF₄
374 lattice has particularly favorable properties [50,51]. The large surface areas of nanoparticles
375 exposes a sizable fraction of the lanthanoid emitters to solvent quenching, so these surface ions
376 are protected from such environmental effects by growing a shell of the host material around the
377 UCNP [52-54]. In addition, silica or polymer coatings can be introduced [55]. The emission
378 properties of a Yb³⁺/Er³⁺ nanomaterial is illustrated in Figure 7. The narrow line and long
379 lifetime luminescence as well as the photostability of such UCNPs make them well suited for
380 biological imaging.

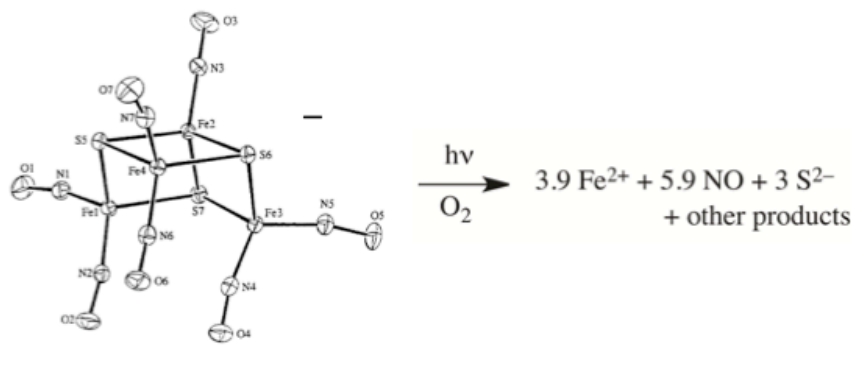


381
382 **Figure 7.** Upconversion emission spectra silica coated UCNPs, Yb/Er (20/2%) in β-NaYF₄ core with a NaYF₄ shell
383 in aqueous solution. The spectra resulting from three different powers (0.58, 0.96 and 1.36 W) of a 980 nm diode
384 laser excitation source indicate a non-linear response of emission intensity to excitation power. A log/log plot of
385 emission intensity at 550 nm vs. power is linear with a slope of 1.63.

386 There have been limited studies with regard to using NIR excitation of UCNPs for uncaging
387 reactions. Several years ago Carling et al. [56] showed that 980 nm photolysis of NaYF₄:Yb/Tm
388 (30/0.5%) nanoparticles surface loaded with 3',5'-(carboxymethoxy)benzoin acetate (CBA) led

389 to cleavage (uncaging) of acetate from this UV absorbing organic chromophore. Similarly, Y.
 390 Yang et al. [57] utilized upconverted Tm^{3+} UV emission from $NaYF_4:Yb/Tm$ (20/0.2%): $NaYF_4$
 391 *core:shell* UCNP to release d-luciferin conjugated to a thiolated silica layer in C6 glioma cells
 392 and in living mice. The latter experiment demonstrates how NIR excitation of UCNP might be
 393 used to deliver bioactive molecules to living systems.

394 We have recently shown [58] that NIR excitation of assemblies based on
 395 $NaYF_4:Yb/Er$ (20/2%): $NaYF_4$ *core:shell* UCNP can trigger NO uncaging from Roussin's black
 396 salt anion $Fe_4S_3(NO)_7^-$ (RBS, Na^+ salt). Solutions of RBS alone are photoactive under
 397 UV/visible excitation (eq. 6) [59,60] but are not affected by NIR irradiation. Notably the strong



399 absorption bands of RBS overlay the visible range emissions of β - $NaYF_4:Yb/Er$ UCNP. Two
 400 RBS/UCNP combinations were prepared. One involved β - $NaYF_4:Yb/Er$ (20/2%): $NaYF_4$
 401 *core:shell* UCNP (average diameter 20 nm) coated with a silica layer (~10 nm) surface modified
 402 with cationic $-NH_3^+$ groups to attract the **RBS** anions. NIR (980 nm) irradiation of these
 403 suspended in a solution of **NaRBS** resulted in the NO generation as detected by a GE Nitric
 404 Oxide Analyzer (NOA). NO output was linear with the irradiation time at constant power but
 405 showed a non-linear response to systematic increases in laser power from 1 to 4.5 W as expected.

406 The second approach is illustrated in Scheme 7. A mesoporous silica layer was added to the
 407 analogous UCNP to give nanomaterials with a porous layer. These were then impregnated with
 408 RBS after which they were coated with poly(allylamine hydrochloride). The RBS remained
 409 encapsulated after washing and isolating these nanocarriers of caged NO. However, NIR
 410 irradiation released NO [58]. The quantum efficiencies for both systems were small, owing to
 411 the low photoreactivity of RBS and the low upconversion yield. Nonetheless, these proof-of-
 412 concept experiments show that UCNP offer the opportunity to deliver NO to specific targets

413 using NIR light generated by a relatively inexpensive diode laser. One can anticipate that the
414 photonic efficiencies will be improved, especially in the context that these nanocarriers offer the
415 opportunity for targeted uncaging of NO at therapeutically relevant sites [51].



416

417 **Scheme 7.** Preparation UCNPs with a mesoporous silica shell impregnated with Roussin's Black Salt (red dots), a
418 photo active nitric oxide generator, and coated with poly(allylamine). NIR irradiation leads to upconversion to
419 wavelengths overlapping the RBS absorbance and NO uncaging (adapted from ref. 58)

420

421 **Summary:**

422 This article has largely summarized studies at UCSB that have explored strategies for
423 photochemical uncaging of the nitric oxide for potential therapeutic applications. Described are
424 studies with NO precursors coupled to antennas consisting of organic dyes or nanoparticles and
425 utilizing both single and multiple photon excitation. The latter type of excitation offers the
426 opportunity to use near-infrared light to access excited states that would otherwise require visible
427 or ultraviolet light. NIR wavelengths are less damaging and will penetrate more deeply into
428 mammalian tissue. The other advantage of multi-photon excitation is the non-linear intensity
429 response of the induced photochemistry that offers the opportunity for three-dimensional
430 resolution. The use of lanthanoid ion doped upconverting nanoparticles as sensitizers for NIR
431 uncaging appears particularly promising given that physiologically relevant concentrations of
432 NO can be uncaged using a continuous NIR diode lasers. The relatively low expense and the
433 ease of operation and maintenance of such lasers would provide considerably greater access than
434 the ultrafast pulsed lasers that were used to generate the intensities needed for simultaneous two
435 photon excitation. Nonetheless, it is clear that moving any such methods from the laboratory
436 benchtop to therapy will be very challenging.

437 **Acknowledgement:** The studies described here have received long-term support from the
438 Chemistry Division of the US National Science Foundation (current grant CHE-1058794). I
439 thank the many graduate, undergraduate and postdoctoral scholars and collaborators who
440 contributed to this research.

441

442 **References:**

- 443 [1] P. C. Ford, J. Bourassa, B. Lee, I. Lorkovic, K. Miranda, L. Laverman, *Coord. Chem. Rev.*
444 **171** (1998) 185-202.
- 445 [2] A. D. Ostrowski, P. C. Ford, *Dalton Trans* (2009) 10660-10669.
- 446 [3] P. C. Ford, *Acc. Chem. Res.* **41** (2008) 190-200.
- 447 [4] R. D. Rimmer, H. Richter, P. C. Ford, *Inorg. Chem.* **49** (2010) 1180 –1185.
- 448 [5] R. D. Rimmer, A. Pierri, P. C. Ford *Coord. Chem. Rev.*, **256**, (2012) 1509-1519.
- 449 [6] A. E. Pierri, A. Pallaoro, G. Wu, P. C. Ford, *J. Am. Chem. Soc.* **134** (2012) 18197-18200.
- 450 [7] L.R. Makings, R. Y. Tsien, , *J. Biol. Chem.* **269** (1994) 6282-6285.
- 451 [8] E. Tfouni, M. Krieger, B. R. McGarvey, D. W. Franco, *Coord. Chem. Rev* **236** (2003) 57-69.
- 452 [9] C. N. Lunardi, A. L. Cacciari, R. S. Silva, L. M. Bendhack, *Nitric Oxide* **15** (2006) 252-258.
- 453 [10] M. J. Rose, P. K. Mascharak, *Coord. Chem. Rev.* **252** (2008) 2093-2114.
- 454 [11] S. Sortino, *Chem. Soc. Rev.* **39** (2010) 2903-2913.
- 455 [12] E. Tfouni, F. G. Doro, A. J. Gomes, R. S. da Silva, G. Metzker, P. G. Zanichelli Benini, D.
456 W. Franco, *Coord. Chem. Rev.* **254** (2010) 355-371.
- 457 [13] U. Schatzschneider, *Inorg. Chim. Acta* **374** (2011), 19-23.
- 458 [14] C. C. Romao, W. A. Bläetler, J. D. Seixas, *Chem. Soc. Rev.* **41** (2012) 3571-3583.
- 459 [15] K. L. Ciesinski, K. J. Franz. *Angew. Chem. Int. Ed.* **50** (2011) 814-824.
- 460 [16] L. A. Ridnour, D. D. Thomas, C. Switzer, W. Flores-Santana, J. S. Isenburg, S. Ambs, D. D.
461 Roberts, D. A. Wink *Nitric Oxide* **19** (2008) 73-76.
- 462 [17] J. B. Mitchell, D. A., Wink, W. DeGraff, J. Gamson, L. K. Keefer, M. C. Krishna, *Cancer*
463 *Res.*, **53** (1993) 5845-5848.
- 464 [18] H. Yasuda, *Nitric Oxide* **19** (2008) 205-216
- 465 [19] T. C. Bellamy, C. Griffiths, J. Garthwaite, *J. Biol. Chem.* **277** (2002) 31801-31807.
- 466 [20] J. Bourassa, W. DeGraff, S. Kudo, D. A. Wink, J. B. Mitchell, P. C. Ford, *J. Am. Chem.*
467 *Soc.* **119** (1997) 2853-2862.
- 468 [21] R. Motterlini, A. Gonzales, R. Foresti, J. E. Clark, C. J. Green, R. M. Winslow, *Circ. Res.*
469 **83** (1998), 568-577.
- 470 [22] L. E. Otterbein, B. S. Zuckerbraun, M. Haga, F. Liu, R. P. Song, A. Usheva, C. Stachulak,
471 N. Bodyak, R. N. Smith, E. Csizmadia, S. Tyagi, Y. Akamatsu, R. J. Flavell, T. R. Billiar, E.
472 Tzeng, F. H. Bach, A. M. K. Choi, M. P. Soares, *Nature Med.* **9** (2003) 183-190.
- 473 [23] R. Motterlini, L. E. Otterbein, *Nature Rev. Drug Discovery* **9** (2010) 728-743
- 474 [24] K. Katada, A. Bihari, S. Mizuguchi, N. Yoshida, T. Yoshikawa, D. D. Fraser, R. F. Potter,
475 G. Cepinskas, *Inflammation* **33** (2010) 92-100.
- 476 [25] Y. Caumartin, J. Stephen, J. P. Deng, D. Lian, Z. Lan, W. Liu, B. Garcia, A. M. Jevnikar, H.
477 Wang, G. Cepinskas, P. P. W. Luke, *Kidney Int.* **79** (2011) 1080-1089
- 478 [26] A. M. Smith, M. C. Mancini, S. Nie, *Nature Nanotech.* **4** (2009) 710-711.
- 479 [27] C. F. Works, P. C. Ford, *J. Am. Chem. Soc.* **122** (2000) 7592-7593.
- 480 [28] M. De Leo, P. C. Ford, *J. Am. Chem. Soc.* **121** (1999) 1980-1981.

- 481 [29] C. L. Conrado, J. L. Bourassa, C. Egler, S. Wecksler, P. C. Ford, *Inorg. Chem.*, **42** (2003)
482 2288-2293.
- 483 [30] C. L. Conrado, S. R. Wecksler, C. Egler, D. Magde, P. C. Ford, *Inorg. Chem.*, **43** (2004)
484 5543-5549.
- 485 [31] S. R. Wecksler, A. Mikhailovsky, D. Korystov, P. C. Ford, *J. Am. Chem. Soc.*, **128** (2006)
486 3831-3837.
- 487 [32] A. D. Ostrowski, R. O. Absalonson, M. A. DeLeo, G. Wu, J. G. Pavlovich, J. Adamson, B.
488 Azhar, A. V. Iretskii, I. L. Megson, P. C. Ford, *Inorg. Chem.* **50** (2011) 4453-4462.
- 489 [33] A. D. Ostrowski, S. J. Deakin, B. Azhar, T. W. Miller, N. Franco, M. M. Cherney, A. J. Lee,
490 J. N. Burstyn, J. M. Fukuto, I. L. Megson, P. C. Ford *J. Med. Chem.* **53** (2009) 715-722.
- 491 [34] F. DeRosa, X. Bu, P. C. Ford *Inorg. Chem.* **44** (2005) 4157-4165.
- 492 [35] D. Neuman, A. D. Ostrowski, A. A. Mikhailovsky, R. O. Absalonson, G. F. Strouse, P. C.
493 Ford *J. Am. Chem. Soc.* **130** (2008) 168-175.
- 494 [36] P. T. Burks, A. D. Ostrowski, A. A. Mikhailovsky, E. M. Chan, P. S. Wagenknecht and P.
495 C. Ford *J. Am. Chem. Soc.* **134** (2012) .
- 496 [37] W. Denk, J. H. Strickler, W. W. Webb, *Science* **248** (1990) 73-76.
- 497 [38] P. T. C. So, C. Y. Dong, B. R. Masters, K. M. Berland, *Annu. Rev. Biomed. Eng.* **2** (2000)
498 399-429.
- 499 [39] B. W. Pedersen, T. Breitenbach, R. W. Redmond, P. R. Ogilby. *Free Rad. Res.* **44** (2010)
500 1383-1397.
- 501 [40] G. S. He, L.-S. Tan, Q. Zheng, P. N. Prasad, *Chem. Revs.* **108** (2008) 1245-1330.
- 502 [41] M. Rumi, S. Barlow, J. Wang, J. W. Perry, S. R. Marder, *Adv Polym Sci.* **213** (2008) 1-95.
- 503 [42] S. Dayal, S., C. Burda, *C. J. Amer. Chem. Soc.* **130** (2008) 2890-2891.
- 504 [43] Y. Liu, P. Chen, Z. H. Wang, F. Bian, L. Lin, S. J. Chang, G. G. Mu, *Laser Physics*, **19**
505 (2009) 1886-1890.
- 506 [44] S. Wecksler, A. Mikhailovsky, P. C. Ford, *P. C. J. Amer. Chem. Soc.* **126** (2004) 13566-
507 13567.
- 508 [45] S. Wecksler, A. Mikhailovsky, D. Korystov, F. Buller, R. Kannan, L.-S. Tan, P. C. Ford,
509 *Inorg. Chem.* **46** (2007) 395-402.
- 510 [46] Q. Zheng, A. Bonoiu, T. Y. Ohulchanskyy, G. S He, P. N. Prasad, *Mol. Pharm.* **5** (2008)
511 389-98.
- 512 [47] S. V. Eliseeva, J.-C. G. Bunzli, *Chem. Soc. Rev.* **39** (2010) 189-227.
- 513 [48] F. Zhang, Y. Wan, T. Yu, F. Q. Zhang, Y. Shi, S. Xie, Y. Li, L. Xu, B. Tu, D. Y. Zhao,
514 *Angew. Chem. Int. Ed.* **46** (2007) 7976-7979.
- 515 [49] F. Wang, X. Liu, *Chem. Soc. Rev.* **38** (2009) 976-89.
- 516 [50] X. Wang, J. Zhuang, Q. Peng, Y. Li., *Nature* **437** (2005) 121-214.
- 517 [51] G. S. Yi, G. M. Chow, *Adv. Funct. Mater.* **16** (2006) 2324-2329.
- 518 [52] A. D. Ostrowski, E. M. Chan, D. J. Gargas, E. M. Katz, G. Han, P. J. Schuck, D. J.
519 Milliron, B. E. Cohen, *ACS Nano* **6** (2012) 2686-2692.
- 520 [53] F. Wang, J. Wang, X. Liu, *Angew. Chem. Int. Ed.* **49** (2010) 7456-7460.
- 521 [54] G.-S. Yi, G.-M Chow, *Chem. Mater.* **19** (2007) 341-343.

- 522 [55] H. S. Qian, H. C. Guo, P. C. L. Ho, R. Mahendran, Y. Zhang, *small* **5** (2009) 2285–2290.
523 [56] C. J. Carling, F. Nourmohammadian, J. C. Boyer, N. R. Branda, *Angew. Chem. Int. Ed.* **49**
524 (2010) 3782–3785.
- 525 [57] Y. Yang, Q. Shao, R. Deng, C. Wang, X. Teng, K. Cheng, Z. Cheng, L. Huang, Z. Liu, X.
526 Liu, B. Xing, *Angew. Chem. Int. Ed.* **51** (2012) 3125–3129.
- 527 [58] J. V. Garcia, J. Yang, D. Shen, C. Yao, X. Li, G. D. Stucky, D. Y. Zhao, P. C. Ford, F.
528 Zhang, *Small*, **8** (2012) 3800–3805
- 529 [59] F. W. Flitney, I. L. Megson, J. L. M. Thomson, G. D. Kennovin, A. R. Butler, *Br. J.*
530 *Pharmacol.*, **117** (1996) 1549-1557.
- 531 [60] J. L. Bourassa, B. Lee, S. Bernard, J. Schoonover, P. C. Ford, *Inorg. Chem.* **38** (1999)
532 2947-2952.
533